

The Slow Wallerian Degeneration Protein, Wld^S, Binds Directly to VCP/p97 and Partially Redistributes It within the Nucleus[□]

Heike Laser,^{*†‡} Laura Conforti,^{†§} Giacomo Morreale,[§] Till G.M. Mack,^{*} Molly Heyer,[§] Jane E. Haley,^{||} Thomas M. Wishart,^{||} Bogdan Beirowski,^{*} Simon A. Walker,[§] Georg Haase,[¶] Arzu Celik,^{*} Robert Adalbert,[§] Diana Wagner,^{*} Daniela Grumme,^{*} Richard R. Ribchester,^{||} Markus Plomann,[#] and Michael P. Coleman^{*§}

^{*}Institute for Genetics and Center for Molecular Medicine, University of Cologne, D-50674 Cologne, Germany; [§]The Babraham Institute, Babraham, Cambridge CB2 4AT, United Kingdom; ^{||}Division of Neuroscience, University of Edinburgh, Edinburgh EH8 9JZ, United Kingdom; [¶]Avenir Team, INSERM U29, INMED, Luminy, 13273 Marseille Cedex 09, France; and [#]Center for Biochemistry and Center for Molecular Medicine Cologne, University of Cologne, D-50931 Cologne, Germany

Submitted May 2, 2005; Revised November 28, 2005; Accepted December 2, 2005
Monitoring Editor: Jeffrey Brodsky

Slow Wallerian degeneration (*Wld^S*) mutant mice express a chimeric nuclear protein that protects sick or injured axons from degeneration. The C-terminal region, derived from NAD⁺ synthesizing enzyme *Nmnat1*, is reported to confer neuroprotection *in vitro*. However, an additional role for the N-terminal 70 amino acids (N70), derived from multiubiquitination factor *Ube4b*, has not been excluded. In wild-type *Ube4b*, N70 is part of a sequence essential for ubiquitination activity but its role is not understood. We report direct binding of N70 to valosin-containing protein (VCP; p97/Cdc48), a protein with diverse cellular roles including a pivotal role in the ubiquitin proteasome system. Interaction with *Wld^S* targets VCP to discrete intranuclear foci where ubiquitin epitopes can also accumulate. *Wld^S* lacking its N-terminal 16 amino acids (N16) neither binds nor redistributes VCP, but continues to accumulate in intranuclear foci, targeting its intrinsic NAD⁺ synthesis activity to these same foci. Wild-type *Ube4b* also requires N16 to bind VCP, despite a more C-terminal binding site in invertebrate orthologues. We conclude that N-terminal sequences of *Wld^S* protein influence the intranuclear location of both ubiquitin proteasome and NAD⁺ synthesis machinery and that an evolutionary recent sequence mediates binding of mammalian *Ube4b* to VCP.

INTRODUCTION

The E4 ubiquitination factor *Ube4b* (or *Ufd2a*) has a 123-amino acid N-terminal region that is essential for ubiquiti-

This article was published online ahead of print in *MBC in Press* (<http://www.molbiolcell.org/cgi/doi/10.1091/mbc.E05-04-0375>) on December 21, 2005.

[□] The online version of this article contains supplemental material at *MBC Online* (<http://www.molbiolcell.org>).

[†] These authors contributed equally to this work.

[‡] Present address: International University Bremen, D-28759 Bremen, Germany.

Address correspondence to: Michael P. Coleman (michael.coleman@bbsrc.ac.uk).

Abbreviations used: DRG, dorsal root ganglion; ERAD, endoplasmic reticulum-associated protein degradation; IVTT, *in vitro* transcription and translation; N16, N-terminal 16 amino acids of *Wld^S* and *Ube4b*; N70, N-terminal 70 amino acids of *Wld^S* and *Ube4b*; *Nmnat1*, nicotinamide mononucleotide adenylyltransferase; *Ube4b*, ubiquitination factor E4b; *Ufd2*, ubiquitin fusion degradation protein 2; UPS, ubiquitin proteasome system; VCP, valosin-containing protein; *Wld^S*, slow Wallerian degeneration gene or protein.

nation activity (Mahoney *et al.*, 2002). It is unclear why this region is essential because it does not contain the U box, and it appears to be absent in invertebrate orthologues that ubiquitinate effectively (Koegl *et al.*, 1999; Hatakeyama *et al.*, 2001; Mahoney *et al.*, 2002; Hoppe *et al.*, 2004; Richly *et al.*, 2005). It is important to understand the molecular mechanism of *Ube4b* because it has a key role in the ubiquitin proteasome system (UPS; Hoppe, 2005), it is neuroprotective in polyglutamine disorders (Matsumoto *et al.*, 2004) and an important candidate gene for neuroblastoma (Krona *et al.*, 2003). Information on the substrates of *Ube4b* is beginning to emerge (Hoppe *et al.*, 2004; Okumura *et al.*, 2004; Spinette *et al.*, 2004; Richly *et al.*, 2005) but there is much still to learn about its regulation.

In the slow Wallerian degeneration mutant mouse (*Wld^S*), 70 amino acids of this essential domain of *Ube4b* form the N-terminus of a chimeric protein that delays Wallerian degeneration of injured axons in mice and rats by 10-fold (see Figure 1A; Lunn *et al.*, 1989; Mack *et al.*, 2001; Adalbert *et al.*, 2005). The chimeric protein is absent in wild-type mice. This sequence (N70) is fused in *Wld^S* protein to the full coding sequence of nicotinamide mononucleotide adenylyltransferase (*Nmnat1*; Conforti *et al.*, 2000; Emanuelli *et al.*, 2001; Mack *et al.*, 2001), implicating the UPS or NAD⁺ metabolism

in regulating axon degeneration. Wld^S also delays axon degeneration in a wide range of neurodegenerative disorders and acute retrograde axonal degeneration after spinal injury, indicating that axon degeneration mechanisms are more closely related than previously thought (Wang *et al.*, 2002; Ferri *et al.*, 2003; Samsam *et al.*, 2003; Coleman, 2005; Kerschensteiner *et al.*, 2005; Mi *et al.*, 2005). Surprisingly, Wld^S in vivo has only been found in nuclei, suggesting that downstream axonal effector(s) mediate its remarkable effect on axon degeneration (Mack *et al.*, 2001; Samsam *et al.*, 2003; Sajadi *et al.*, 2004).

Nmnat1 activity was reported to preserve injured axons for 3 d in vitro (Araki *et al.*, 2004; Wang *et al.*, 2005). However, axons in vivo are far longer, have a profoundly different environment, and are protected by full-length Wld^S for up to 3 wk (Crawford *et al.*, 1995; Adalbert *et al.*, 2005). A contribution of N70 to strengthening the neuroprotective phenotype in vivo is suggested by the fact that transgenic mice overexpressing Nmnat1 show a normal rate of Wallerian degeneration (Coleman and Perry, 2002; Conforti and Coleman, unpublished data). N70 could contribute to neuroprotection by perturbing the UPS, which is important for regulating axon degeneration (Zhai *et al.*, 2003; Macinnis and Campenot, 2005). Alternatively, it could influence intranuclear targeting of Nmnat1, with its intrinsic NAD⁺ synthesis activity, as Wld^S protein clusters to discrete intranuclear foci in skeletal muscle (Mack *et al.*, 2001) and in many neuronal subtypes in vivo (Haley *et al.*, unpublished results). The inability of successive investigators to detect any increase in NAD⁺ level when Nmnat1 is manipulated (Mack *et al.*, 2001; Anderson *et al.*, 2002; Araki *et al.*, 2004) suggests that NAD⁺ is synthesized at highly localized intranuclear sites or immediately is passed to downstream components within the same complex. Either way, intranuclear targeting should be important.

To understand better the function of N70 in both Wld^S and Ube4b proteins, we sought N70 binding partners. We identified valosin containing protein (VCP) as a direct binding partner of N70 that becomes targeted to discrete intranuclear foci when Wld^S protein is present. VCP, one of the AAA family of ATPases associated with a variety of activities, has critical roles in the UPS (Dai and Li, 2001; Jarosch *et al.*, 2002; Wang *et al.*, 2004) and many other cellular roles dictated by interacting proteins (Meyer *et al.*, 2000; Mogk *et al.*, 2004; Wang *et al.*, 2004). It accumulates in neuronal nuclei in a range of neurodegenerative diseases and can influence neurodegeneration both positively and negatively (Hirabayashi *et al.*, 2001; Higashiyama *et al.*, 2002; Mizuno *et al.*, 2003; Watts *et al.*, 2004; Schroder *et al.*, 2005). Its intranuclear roles include interaction with Werner protein to influence the DNA damage response pathway (Indig *et al.*, 2004) and the nuclear import of the T-cell-specific adaptor protein (Marti and King, 2005). Our data suggest the possibility of further intranuclear roles for VCP and an important function for the N70 domain in both wild-type Ube4b and Wld^S proteins.

MATERIALS AND METHODS

Constructs

VCP full-length cDNA was PCR-amplified with the Expand High Fidelity PCR System (Roche, Mannheim, Germany) from a mouse fibroblast cDNA library (kindly provided by R. Lange) using the 5' BamHI- and 3' SalI-tagged primers (restriction sites in bold): 5'-ATATATGGATCCCATGGCCCTCTG-GAGCCGATTC-3'; 5'-AATATTGTCGACTTAGCCATACAGTCCATCGTC-3'.

The products were cloned with BamHI/SalI into pGEX5X-1 (Amersham Biosciences, Freiburg, Germany), and with NcoI/SalI into the pGBKT7 vector (BD Biosciences Clontech, Heidelberg, Germany). The Wld^S protein, N70 and further truncation products were similarly PCR-amplified and cloned using the Wld^S transgene construct (Mack *et al.*, 2001) as template and appropriate

primers based on the Wld^S cDNA (GenBank AF260924). Human Ube4b was amplified from a construct kindly provided by Professor James Mahoney using primers 5'-ATCCCGGAATTCATGGAGGAGCTGAGCGCTGAT-3' and 5'-CCGCCTCGAGTTAGTGATCGCTGTCTGTTT-3' (*EcoRI* and *XhoI* sites for cloning into pGEX5X-1 in bold). cDNA sequence encoding full-length Wld^S protein, Nmnat-1 or Ube4b amino acids 1-70 (N70) was PCR-amplified from the Wld^S transgene template (Mack *et al.*, 2001) using the high-fidelity enzyme Pfu (Stratagene, Heidelberg, Germany) and appropriate combinations of the following primers (1 + 2, 4 + 2, and 1 + 3, respectively). 5' restriction enzyme tags, added for cloning purposes, are shown in bold and the first or last three bases of sequence derived from the Wld^S gene are underlined. A single base change to repress the stop codon of Wld^S Rev and allow read-through of the C-terminal EGFP is double-underlined: 1) 5'-TAGATCCCAAGCTTAACTTTCACCATTAAAGAGGAAAGCGATG-3'; 2) 5'-GCGGGATCCCGTCCAGAGTGGG-ATGGTTGTG-3'; 3) 5'-TCTTCCCCGGGCTCTGCTGCACCTATGGGGGA-3'; and 4) 5'-GACTAGCTAGCATGGACTCATCCAAGAAGACAG-3'.

After cloning of pEGFP-N1 (BD Biosciences), all sequences were verified using the Taq FS BigDye-terminator cycle sequencing method on a ABI 377 prism sequencer and the corresponding ABI software. The sequences were analyzed using the GCG program Wisconsin Package Version 10.2 (Accelrys, San Diego, CA).

Full-length Wld^S DsRed construct was generated by cloning the HindIII/BamHI insert from pEGFP-N1 (above) into pDsRed2-N1 (BD Biosciences). Wld^S lacking N16 was generated using the following HindIII and BamHI-tagged primers: 5'-TAGCCCAAGCTTATAGCCGCCACCATGCTGTGCTG-TGGACAGACCT-3'; 5'-GCGGGATCCCGTCCAGATGGGAATGGTTG-3'.

Pulldown Assays

C57BL/6J mouse brain homogenates were used in this experiment to avoid competition from endogenous Wld^S protein. Brains were flash-frozen and homogenized in 50 volumes of 50 mM Tris, pH 9.0, and 1% deoxycholate containing protease inhibitor mix (Sigma, Taufkirchen, Germany). After incubating for 30 min at 37°C, insoluble material was removed by centrifugation (10,000 × g, 30 min) and the supernatant was dialyzed against binding buffer (50 mM Tris, pH 7.4, and 0.1% Triton X-100) overnight at 4°C. Homogenates were incubated overnight at 4°C with GST fusion proteins bound to glutathione Sepharose 4B. The beads were washed four times with phosphate-buffered saline (PBS)/0.1% Triton X-100 and resuspended in 3× standard Laemmli sample buffer. Proteins were separated by SDS-PAGE on 12% gels and analyzed by Western blotting.

MALDI-TOF Mass Spectrometry

Proteins fished by a pulldown assay were eluted with double-concentrated SDS-PAGE sample buffer and separated by SDS-PAGE. From the gel individual Coomassie blue-stained protein bands were excised with a scalpel and destained by washing with 25 mM NH₄HCO₃/50% acetonitrile. For MALDI-TOF mass spectrometry analysis, the samples were dissolved in 5 μl 0.1% aqueous trifluoroacetic acid. MALDI-MS was carried out in linear mode on a Bruker Reflex IV equipped with a video system (Rheinstetten, Germany), a nitrogen UV laser (Omax = 337 nm), and a HiMass detector. One microliter of the sample solution was placed on the target and 1 μl of a freshly prepared saturated solution of sinapinic acid in acetonitrile/H₂O (2:1) with 0.1% trifluoroacetic acid was added. The spot was then recrystallized by addition of another 1 μl acetonitrile/H₂O (2:1), which resulted in a fine crystalline matrix. For recording of the spectra an acceleration voltage of 20 kV was used, and the detector voltage was adjusted to 1.9 kV. Approx. 500 single laser shots were summed into an accumulated spectrum. Calibration was carried out using the single and doubly protonated ion signal of bovine serum albumin for external calibration. Identification of the mass fingerprint spectra was performed using the Mascot program available from Matrix Science on the World Wide Web (<http://www.matrixscience.com/home.html>).

Isolation and Immunoprecipitation of Nuclear Proteins

Six mouse brains (ca. 2.5 g) were each homogenized using a Dounce homogenizer in 40 ml precooled nuclear isolation medium (NIM; 0.25 M sucrose, 25 mM KCl, 5 mM MgCl₂, 10 mM Tris/HCl, pH 7.4) supplemented with protease inhibitor cocktail (Sigma). Unbroken cells and connective tissue were removed by filtration. The filtered homogenate was then diluted with an equal volume of ice-cold NIM, centrifuged (10 min, 800 × g) and the pellet, including lipids, was resuspended in 40 ml NIM supplemented with protease inhibitor cocktail. After repeating the centrifugation, the new pellet was resuspended in 8 ml NIM, 2 ml sucrose density barrier (SDB; 2.3 M sucrose, 25 mM KCl, 5 mM MgCl₂, 10 mM Tris/HCl, pH 7.4) solution was added and mixed thoroughly. 10 ml of the suspension was underlayered with 2.3 M sucrose and centrifuged for 1 h at 100,000 × g in a Beckman SW41 Ti rotor (Krefeld, Germany). The pellet, together with remaining lipids, was resuspended in PBS containing 1% Triton X-100 and incubated for 2 h at 4°C with continuous agitation. Samples were then centrifuged at 16,000 × g to generate a supernatant containing solubilized nuclear proteins.

For the subsequent immunoprecipitation, protein lysates were preincubated with 30 μl of protein G agarose (Roche) for 2 h at 4°C under constant

agitation. Samples were centrifuged (5 min, 500g) to remove proteins unspecifically bound to the protein G agarose and 3 μ l of anti-Wld^S rabbit serum and another 30 μ l of protein G agarose were then added and incubated overnight at 4°C with constant agitation. The precipitated proteins bound to protein G agarose were then repeatedly washed by centrifugation at 500 \times g at 4°C for 5 min. The final pellet was resuspended in 1 ml PBS, 1% Triton X-100. Samples were then analyzed by SDS-PAGE and immunoblotting.

In Vitro Binding Assays

GST fusion proteins were purified and coupled to glutathione-Sepharose 4B according to the protocol of the manufacturer (Amersham Biosciences). The pGBKT7 constructs containing the T7 promoter were in vitro transcribed and translated incorporating ³⁵S-methionine using the TNT T7 Reticulocyte Lysate Coupled Transcription/Translation kit from Promega (Promega GmbH, Mannheim, Germany). The obtained proteins were mixed with equal amounts of GST fusion proteins and the binding assay was performed as previously described (Dai *et al.*, 1998). Reactions were analyzed by SDS-PAGE, and the gel was fixed with 10% methanol/10% acetic acid before autoradiography. Purified His-tagged VCP was a kind gift from Dr. Sarah Spinette (Johns Hopkins).

Cell Culture and Transfection

Plasmid DNA was isolated using the endonuclease free plasmid kit (QIAGEN, Hilden, Germany). DNA was transfected using LipofectAMINE 2000 (Invitrogen) into COS-7, PC12, or HeLa cells immediately before differentiation by culturing in 100 ng/ μ l NGF on a type IV collagen substrate (Sigma). The "TV" PC12 subline, stably transfected with a tet-off inducible C-terminal EGFP-tagged VCP construct (Kobayashi *et al.*, 2002) was grown in 1.0 μ g/ml doxycycline (Sigma), which was removed to induce VCP/EGFP expression. Protein location was observed 1–5 d after transfection. Spinal motor neurons from embryonic day 14 (E14) embryonic rats were cultured and electroporated in suspension as previously described (Henderson *et al.*, 1995; Raoul *et al.*, 2002).

Immunocytochemistry

Slices of 100 μ m were cut from the cerebellum of Wld^S mice and fixed in 4% paraformaldehyde (Fisher, Schwerte, Germany). Lumbar spinal cord dorsal root ganglia (DRG) were removed from Wld^S mice or rats and fixed in 4% paraformaldehyde, and then 20- μ m sections cut on a cryostat. Slices were incubated for 2 h at room temperature in serum blocker consisting of 4% bovine serum albumin (Sigma) and 0.5% Triton X-100 (Sigma) in PBS. Wld-18 antibody (Samsam *et al.*, 2003; 1:500 dilution) plus VCP antibody (against amino acids 9–130; BD Biosciences; 1:200 dilution; or mouse monoclonal to VCP (ab11433); AbCam, Cambridge, United Kingdom, 1:500 dilution) were applied simultaneously in serum blocking solution overnight at 4°C. After washing with PBS, slices were incubated overnight at 4°C in a solution containing TRITC-conjugated anti-rabbit (DAKO, Hamburg, Germany; 1:20 dilution in PBS) plus Alexa488-conjugated anti-mouse (Molecular Probes, Leiden, Netherlands; 1:200) secondary antibodies. Slices were then washed in PBS and incubated in To-pro3 (Molecular Probes) for 10 min before mounting in Mowiol/DABCO preparation. Staining was visualized on a laser scanning confocal microscope (Bio-Rad Radiance 2000, Hemel Hempstead, United Kingdom) and Z-series were merged using Lasersharp (Bio-Rad) software.

Cultured cells were fixed for 30 min in 4% paraformaldehyde, permeabilized with Triton-X-100 (0.1%, 5 min), blocked with horse serum (5%, 1 h), and incubated with primary (1 h) and secondary (45 min) antibodies with multiple washes in PBS between each stage.

VCP antibody was used as described above. Anti-ubiquitin polyclonal antibody (DAKO) was used at 1:100 dilution and anti-neurofilament medium chain polyclonal antibody (Chemicon, Hofheim, Germany; Ab1987) was used as 1:1000. Images were taken on a Zeiss LSM 510 META confocal system (Oberkochen, Germany; LSM Software Release 3.2) coupled to a Zeiss Axiovert 200 microscope.

Western Blotting

Wld^S protein expression was analyzed in mouse cerebella homogenized in five volumes of RIPA buffer, respectively, plus 1 \times Complete protease inhibitor cocktail (Roche) or in PC12 cells scraped from the dish in a minimal volume of the same buffer. Proteins were separated by SDS-PAGE and semidry blotted onto nitrocellulose (Bio-Rad). Blocking and incubation with primary antibodies and horseradish peroxidase-conjugated secondary antibodies (1:5000; Serotec, Heidelberg, Germany) were performed in PBS plus 0.02% Tween-20 and 5% low fat milk. Proteins were visualized using the ECL detection kit (Amersham Biosciences) according to the manufacturer's instructions.

RESULTS

Wld^S Protein Binds Directly to VCP through its N-terminal Domain

A screen for Wld^S binding partners revealed that a protein of ca. 97 kDa can be pulled down in large quantities from

mouse brain homogenate by GST-Wld^S (Figure 1B). N70 is sufficient for this activity. Isolation of this protein from an SDS-PAGE gel followed by MALDI-TOF mass spectrometry protein identification revealed several tryptic peptides exactly matching sequences from murine VCP (Figure 1C). To confirm that binding of Wld^S to VCP is biologically relevant, we coimmunoprecipitated VCP specifically from nuclear extracts of Wld^S mouse brain using antibody Wld-18 and confirmed the identity of VCP by Western blotting (Figure 1D). VCP could not be coimmunoprecipitated from wild-type mouse brain, which lacks Wld^S protein. The reciprocal coimmunoprecipitation was inconclusive because VCP itself was not immunoprecipitated by the BD Biosciences anti-VCP antibody, but these data strongly suggest that the Wld^S/VCP complex is biologically relevant. To determine whether the binding was direct or mediated by other factors, we precipitated purified His-tagged VCP (a kind gift from Dr. Sarah Spinette and Prof. Antony Rosen, Johns Hopkins) using GST-tagged N-terminal fragments of Wld^S (Figure 1E; see also Figure 3). The ability of Wld^S-derived peptides to precipitate VCP was retained in the absence of other relevant proteins, showing that VCP binds directly to the shared N-terminus of Wld^S and Ube4b. Because Wld^S protein has been suggested to alter the UPS (Zhai *et al.*, 2003; Coleman and Ribchester, 2004), we then tested by Western blotting of Wld^S and wild-type brain homogenates whether Wld^S alters turnover of VCP, and thus its steady-state level, and found that it does not (Figure 1F). Thus, VCP directly binds to Wld^S protein through its N70 domain, and this binding does not significantly alter steady-state level of VCP in brain.

Wld^S Colocalizes with and Partially Redistributes VCP

To investigate further whether Wld^S/VCP complexes form inside living cells, we carried out colocalization studies in vitro and in vivo. We took advantage of the fact that Wld^S clusters into discrete intranuclear foci in some neuronal subtypes (Haley *et al.*, unpublished results) and other cells (Mack *et al.*, 2001; Figure 2). After transient transfection of Wld^S/EGFP fusion construct into PC12 cells, VCP partially shifted from the widespread nuclear and cytoplasmic distribution that was previously described (Hirabayashi *et al.*, 2001; Kobayashi *et al.*, 2002) and is present in untransfected cells (Figure 2B, arrow) to produce the same pattern of intranuclear foci as Wld^S (Figure 2B, arrowhead). VCP is an abundant protein (Dai and Li, 2001), so the wider nuclear and cytoplasmic pool remained without any obvious depletion (Figure 2, A–C). VCP was also partially redistributed by Wld^S in HeLa cells which, like PC12, remained healthy (Supplementary Figures 2 and 4).

To study this in vivo, we made use of the finding that cerebellar granule cells and molecular layer neurons also show intranuclear foci of Wld^S protein, albeit of different size and number from PC12 cells (Haley *et al.*, unpublished results). Again Wld^S and VCP colocalized within intranuclear foci in these neurons from Wld^S mice (Figure 2, D–F), whereas in wild-type cerebellum, there were no intranuclear VCP foci (Figure 2, G–I). Some DRG neurons in both Wld^S mice and rats also showed good colocalization (Supplementary Figure 5), indicating that the Wld^S/VCP interaction occurs in at least some neurons known to express the neuroprotective Wld^S phenotype and that this binding is conserved between species. The situation is less clear in motor neurons, where Wld^S is more homogeneously distributed in vivo (Mack *et al.*, 2001; Samsam *et al.*, 2003), and VCP colocalization with Wld^S spots was not evident in vitro (Supplementary Figure 5). Nevertheless, the data are sufficient to conclude that Wld^S and VCP bind one another under phys-

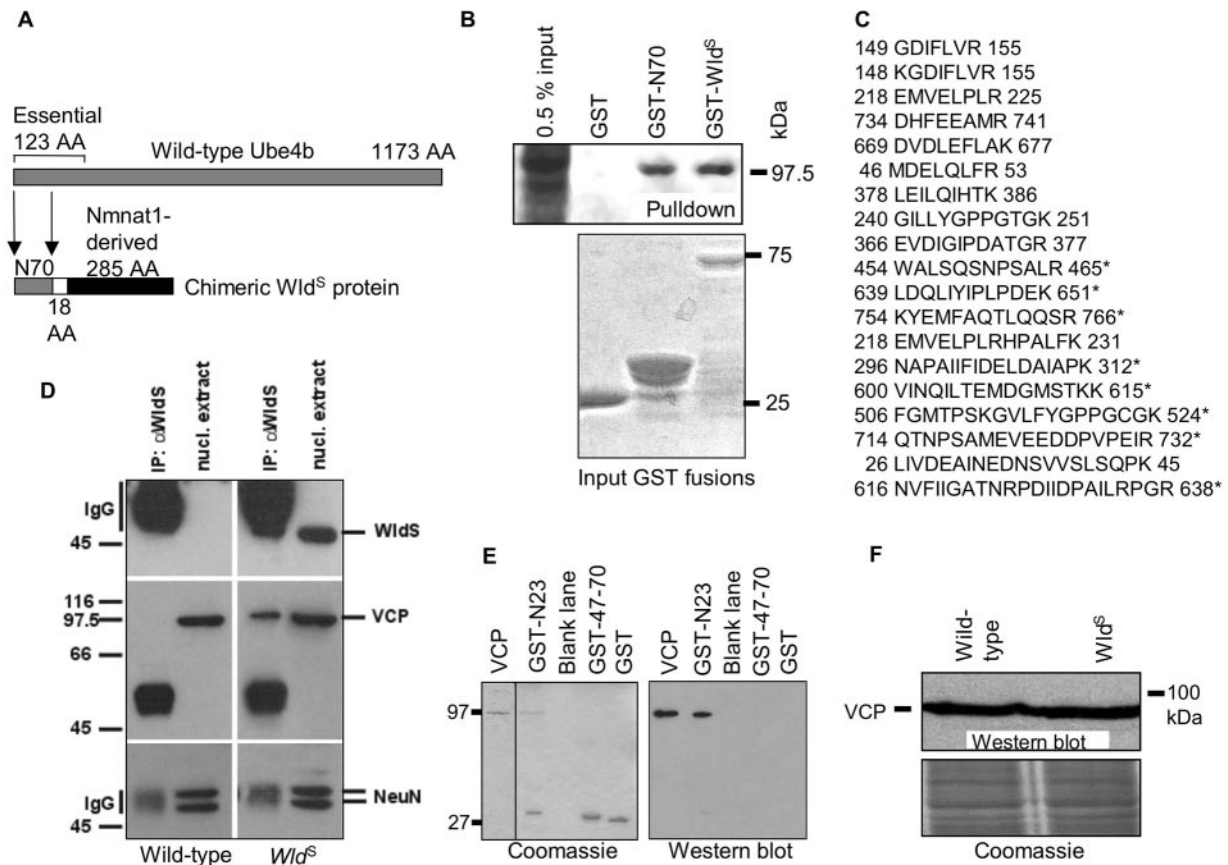


Figure 1. Direct binding of Wld^S/N70 sequence to VCP. (A) The N-terminal 70 amino acids of murine Ube4b (N70) are incorporated into the neuroprotective, chimeric Wld^S protein, fused in-frame to the entire coding sequence (285 amino acids) of Nmnat1 and an 18-amino acid linking region. In wild-type Ube4b, N70 forms part of a 123-amino acid sequence that is essential for ubiquitination activity. (B) A protein of ca. 97 kDa was pulled down from wild-type mouse brain by GST-Wld^S and by GST-N70. Bottom panel, a Coomassie-stained gel of the amounts of each protein used for pulldown, except that the GST sample has been diluted 1:10. The larger N70 and Wld^S proteins were obtained in lower quantities but were still able to precipitate significant amounts of the 97-kDa protein. (C) Tryptic peptides of VCP were identified by MALDI-TOF. Peptides marked with an asterisk (*), plus three additional VCP peptides (unpublished results), were present both in the protein pulled down by N70 and in the one pulled down by Wld^S. (D) Coimmunoprecipitation of VCP with Wld^S protein. Antibody Wld-18 was able to immunoprecipitate Wld^S protein (top) from nuclear extracts of mutant mouse brain (right) but not from wild-type mouse brain (left). Coimmunoprecipitation of VCP showed the same pattern (middle), whereas control protein NeuN is not coimmunoprecipitated (bottom) showing that the VCP result is specific. (E) Evidence that VCP binds directly to the N-terminus of Wld^S and Ube4b. Left, Coomassie-stained gel showing purified VCP and its precipitation by Wld^S peptides; right, Western blot confirming identity of the precipitated VCP and its complete absence in control lanes. The N-terminal 23 amino acids (N23) fused to GST (see also Figure 3) are able to precipitate purified His-tagged VCP. Neither GST alone, nor amino acids 47–70 possess this specific binding activity. (F) VCP Western blot of wild-type and Wld^S mouse brain homogenates showing that steady state levels of VCP are not altered by the presence of Wld^S. Below: Coomassie stain showing equal loading. D–F are representative of at least two experiments.

iological conditions, including in at least some neurons that display the Wld^S phenotype.

VCP Binds within the First 16 Residues of Wld^S

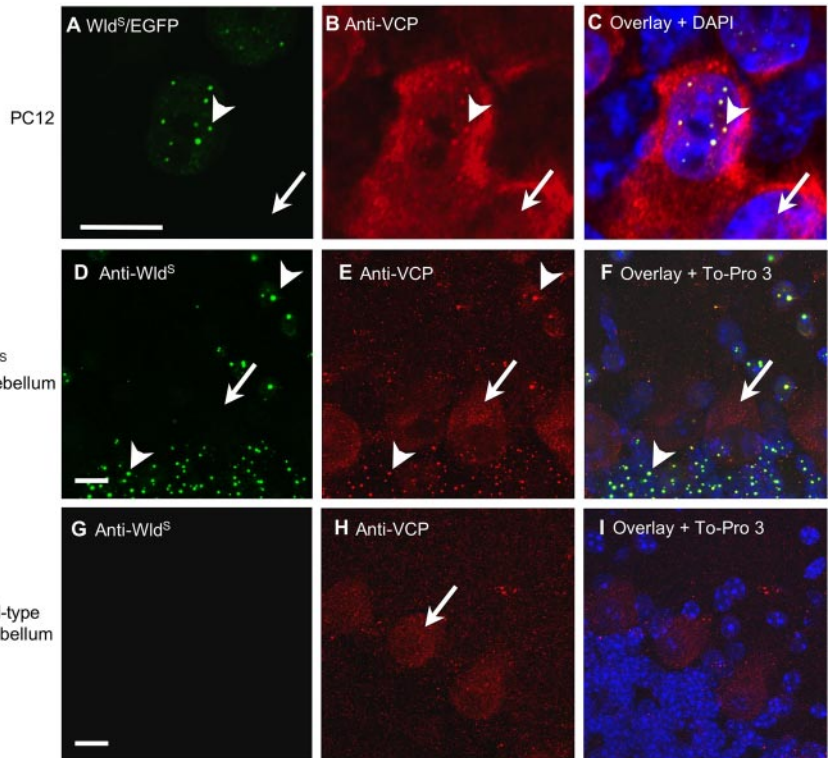
We show above that Wld^S binds to and partially redistributes VCP. To establish that binding causes redistribution, we mapped and then deleted key residues of Wld^S required for VCP binding. Truncated N70 constructs were expressed as GST-fusion proteins and used to pull down IVTT-expressed VCP. First the N-terminal 23 amino acids were found to be necessary and sufficient for VCP binding, and this was subsequently narrowed to the N-terminal 16 amino acids (N16; Figure 3A). Ube4b lacking this sequence also did not bind VCP. Two Wld^S/DsRed2 constructs were then made: one full-length and one lacking N16, and transiently transfected into the TV PC12 stable subline that expresses VCP/EGFP fusion protein in a tet-off-inducible manner (a kind gift from

Prof. Akira Kakizuka). Full-length Wld^S/DsRed2 was able to bring about partial redistribution of VCP/EGFP into intranuclear foci in transfected cells (arrowhead; Figure 3, B–E) but removal of N16 containing the VCP binding site prevented this (Figure 3, F–I). Interestingly, the ability of Wld^S protein to accumulate in intranuclear foci does not require binding to VCP (Figure 3F). Thus, VCP has to bind Wld^S N16 to be partially redistributed in the manner we describe.

The Sequence Targeting Wld^S Protein to Intranuclear Foci Is Not Nmnat1

Because VCP binding is not required to target Wld^S to intranuclear foci, we asked whether this is a property of the Nmnat1 sequence by fusing Nmnat1 to EGFP and transiently transfecting it (Figure 4). Nmnat1, but not N70, was restricted to the nucleus, confirming previous reports that

Figure 2. Wld^S partially relocates VCP in vitro and in vivo. (A–C) PC12 cells transiently transfected with Wld^S/EGFP fusion construct. (A) Wld^S/EGFP shows a punctate intranuclear pattern in transfected cells (arrowhead). Arrow marks nucleus of an untransfected cell. (B) VCP immunocytochemistry reveals the same pattern of intranuclear foci in transfected cells (arrowhead) together with widespread nuclear and cytoplasmic staining. Untransfected cells show only the wider nuclear and cytoplasmic signal (arrow). (C) Overlay, together with DAPI stain, confirms that the Wld^S and VCP puncta colocalize within nuclei. The specificity of the staining and the healthy status of the cells is demonstrated in Supplementary Figures 1 and 3. (D–I) Double immunofluorescence staining of sections of Wld^S and wild-type mouse cerebellum with Wld^S (green) and VCP (red). (D) As in PC12 cells, Wld^S localizes in mouse cerebellar granule cells and molecular layer neurons to intranuclear spots, although there are fewer spots per nucleus than in most PC12 cells (arrowheads). Purkinje cells (arrow) appear not to express Wld^S. (E) Immunostaining for VCP reveals the same pattern of spots as Wld^S (arrowheads), as well as staining both cytoplasm and nuclei of the large Purkinje cells (arrow). (F) Overlay, together with To-pro3 nuclear stain (blue), confirms that the Wld^S and VCP puncta colocalize within nuclei. (G) Wld^S antibody showed no specific stain in wild-type cerebellum. (H) VCP intranuclear foci were not found in cerebellar granule cells or molecular layer neurons in wild-type mice. The faintly stained Purkinje cells (arrow) confirm that E and H were similarly processed and that cells were healthy. (I) Overlay, together with To-pro3 stain, indicates the position of nuclei that lack Wld^S protein. The nonhomogeneous staining by DAPI in C and to-pro3 in F and I reflects nonhomogeneous distribution of heterochromatin (Wu *et al.*, 2005). Scale bars, 10 μ m. Each figure is representative of four or more experiments.



Nmnat1 is a nuclear protein and suggesting that nuclear targeting of Wld^S protein is due to the putative nuclear localization signal of Nmnat1 (Raffaelli *et al.*, 2002; Araki *et al.*, 2004; Magni *et al.*, 2004). However, unlike Wld^S/EGFP, intranuclear distribution of Nmnat1/EGFP was homogeneous apart from its exclusion from nucleoli. The fraction of N70/EGFP that entered the nucleus was also homogeneously distributed, suggesting that Wld^S protein is targeted to intranuclear foci either by a conformational structure involving both N70 and Nmnat1 sequence or by the short unique sequence that separates these two parts of the protein. Cell and nuclear shape indicated that the cells were healthy in all cases. We conclude that Nmnat1 and Wld^S protein differ in their intranuclear distribution, but as shown above, their differing abilities to bind VCP do not underlie this difference.

Wld^S Also Can Partially Relocalize Ubiquitin inside the Nucleus

VCP binds long ubiquitin chains (Dai and Li, 2001) so one consequence of its partial redistribution by Wld^S protein could be redistribution of bound polyubiquitinated proteins. This was supported by immunocytochemistry of PC12 cells transiently transfected with Wld^S/EGFP fusion construct (Figure 5, A–H). As with VCP, the normal distribution of ubiquitin throughout the nucleus and cytoplasm of untransfected cells is joined by a punctate intranuclear pattern in transfected cells, where ubiquitin puncta colocalize with Wld^S/EGFP. Cell and nuclear shape indicated that the cells were healthy (see also Supplementary Figure 3). The asso-

ciation of ubiquitin epitopes with Wld^S also depended on the N16 sequence, suggesting it is secondary to VCP binding to Wld^S (Figure 5, I–P).

An alternative explanation for the accumulation of ubiquitin epitopes at these sites could be ubiquitination of the Wld^S/EGFP fusion protein, so we looked for these putative ubiquitinated species by Western blotting (Figure 6). Wld-18 antibody detected only a single band of the expected size, even on long-exposure ECLs after a generalized accumulation of ubiquitination products due to proteasome inhibition. The intensity of the Wld^S band did increase after proteasome inhibition, suggesting that Wld^S protein is degraded by the UPS but despite this, ubiquitinated Wld^S did not reach detectable levels on the Western blots. Although we cannot rule out the possibility that ubiquitinated Wld^S contributes to the ubiquitin speckles, the inability to detect this putative species on a Western blot and the probable dependence on VCP binding suggest that putative ubiquitination of Wld^S is unlikely to be the sole explanation for the ubiquitin speckles. Thus, we propose that polyubiquitinated proteins may accumulate in the Wld^S/VCP complex.

VCP Binding to N16 Is an Evolutionary “Recent” Development

An alignment of human Ube4b with known orthologues shows that an N-terminal extension containing the N16 sequence is present in mammals, birds, fish, and insects, but this entire region is absent in nematodes, slime molds, and yeasts (Figure 7). Nevertheless, the VCP ortholog Cdc48

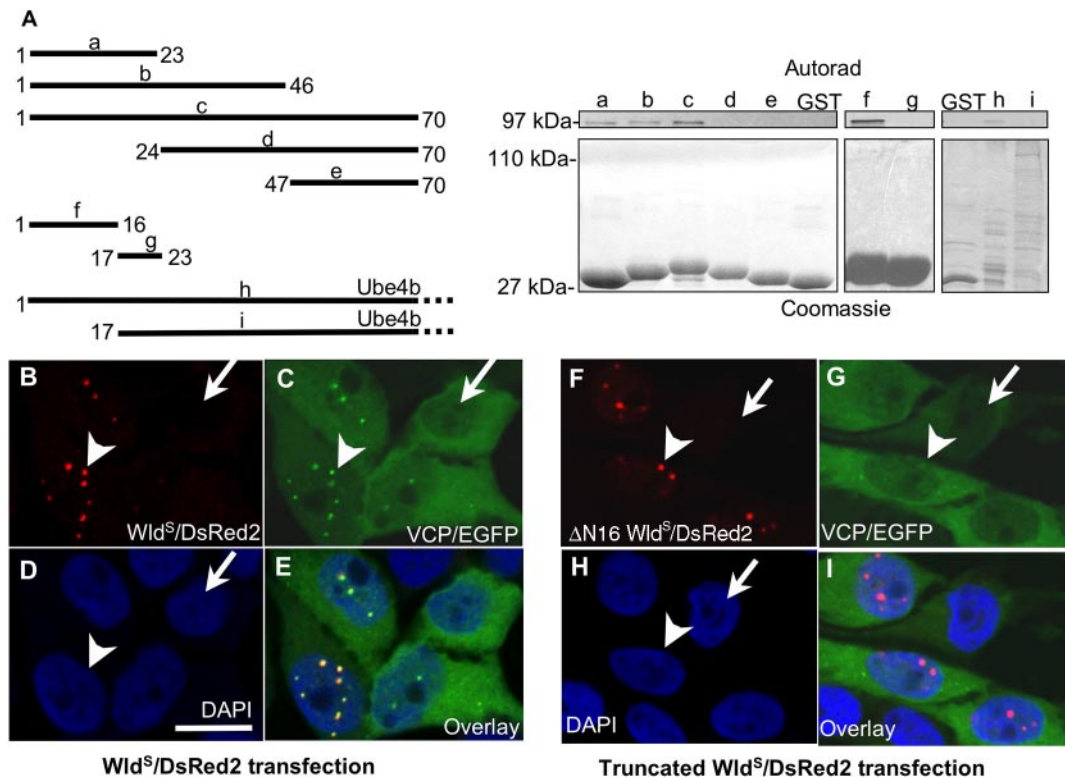


Figure 3. VCP binds within the first 16 residues of Wld^S. (A) Left: truncated GST fusion constructs of Wld^S and Ube4b. Right top, autoradiogram of ³⁵S-labeled, IVTT expressed VCP pulled down with these constructs; right bottom, corresponding Coomassie-stained gel. Constructs a, b, and c, containing the first 23 residues, were able to pull down VCP, but the more C-terminal constructs d and e were not. The region necessary and sufficient for binding was subsequently narrowed to amino acids 1–16 using constructs f and g. Ube4b also pulled down VCP but failed to bind when this sequence was removed. Note that very little soluble full-length GST-Ube4b could be recovered by this method. However, this was sufficient to pull down VCP (lane h), whereas a greater amount of truncated GST-Ube4b (lane i) was not. (B–E) Full-length Wld^S/DsRed2 fusion protein partially redistributes VCP/EGFP fusion protein in the PC12 subline TV. (B) Transiently transfected Wld^S/DsRed2 fusion protein. (C) Stably transfected VCP/EGFP fusion protein. (D) DAPI. (E) Overlay. In cells not transfected by Wld^S/DsRed2, VCP/EGFP (arrow in C), like endogenous VCP (Supplementary Figure 6), is expressed throughout the cytoplasm and most of the nucleus as previously reported (Hirabayashi *et al.*, 2001; Kobayashi *et al.*, 2002). In cells transfected by Wld^S/DsRed2, VCP/EGFP signal colocalizes with the punctate intranuclear pattern of Wld^S/DsRed2 (arrowheads in B and C), while retaining the cytoplasmic and nuclear VCP signal. (F–I) Wld^S/DsRed2 fusion protein truncated by 16 amino acids at the N-terminus does not alter VCP distribution. (F) Transiently transfected, N-terminally truncated Wld^S/DsRed2 fusion protein. (G) Stably transfected VCP/EGFP fusion protein. (H) DAPI. (I) Overlay. VCP/EGFP distribution in the absence of truncated Wld^S/DsRed2 is similar to that in C (arrow in G). Although truncated Wld^S/DsRed2 still shows a punctate intranuclear distribution (arrowhead in F), it does not alter the distribution of VCP/EGFP (arrowhead in G). Scale bar, 10 μ m. Figures are representative of two (A) or three (B–I) experiments.

does bind Ufd2 in *Saccharomyces cerevisiae* (Koegl *et al.*, 1999; Richly *et al.*, 2005) and *Caenorhabditis elegans* (C. Kähler and T. Hoppe, personal communication) so the interaction in these species must have a different molecular basis. The Cdc48 binding site in *S. cerevisiae* has been mapped (Richly *et al.*, 2005) and mammals do have a sequence homologous to it. However, this sequence appears to be insufficient for VCP binding in human, because N-terminally truncated Ube4b did not bind VCP (Figure 3A). Mammalian Ube4b was previously reported to bind VCP (Meyer *et al.*, 2000; Kaneko *et al.*, 2003) but the interacting sequence was not fully mapped. Our data show that VCP binds to N16, and this appears to be a recent event in evolutionary terms with distantly related higher eukaryotes employing a different mode of interaction.

DISCUSSION

We report direct binding between VCP and the N-terminal 16 amino acids of Wld^S protein (N16) that drives partial

redistribution of VCP in nuclei in vivo and in vitro when full-length Wld^S is present. N16 is necessary and sufficient for VCP binding and is necessary for relocation of VCP, but is not required to target Wld^S to discrete intranuclear foci. Thus, sequences outside N16 cause Wld^S to accumulate at these sites and VCP is redistributed through binding to N16. The N-terminal domain of Wld^S also influences the intranuclear distribution of the covalently attached Nmnat1 sequence and hence the distribution of nuclear NAD⁺ synthesis machinery.

A recent report indicates that Nmnat1, but not N70, is sufficient to confer a Wld^S-like phenotype on neurons in vitro (Araki *et al.*, 2004). However, the relative strengths of the neuroprotective phenotypes induced by Nmnat1 and Wld^S were not tested and Nmnat1 was not shown to protect in vivo, where Wld^S robustly protects longer axons for far greater time periods (Mack *et al.*, 2001; Adalbert *et al.*, 2005). Our data show that N70 is not an inert addition to Nmnat1, but instead concentrates VCP, NAD⁺ synthesis activity and probably its associated ubiquitinated proteins into sub-

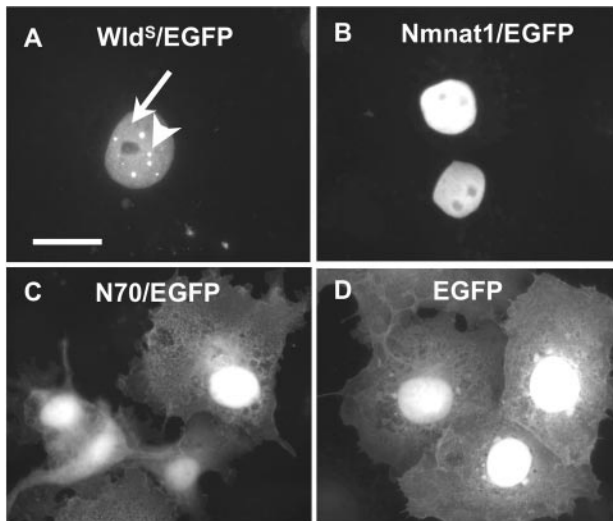


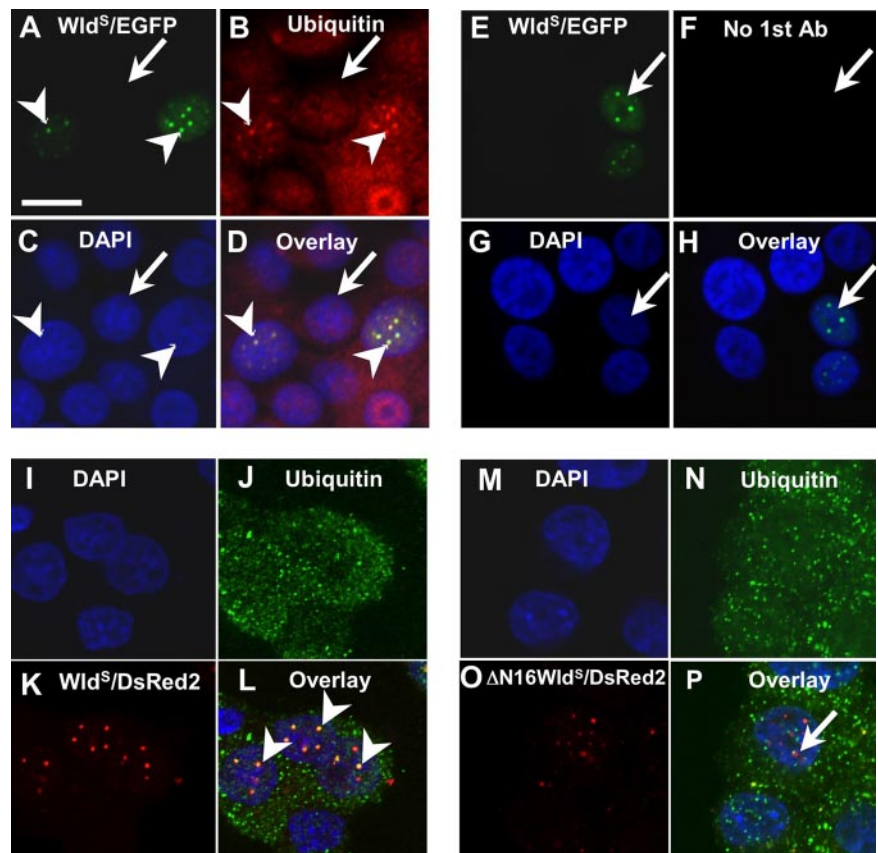
Figure 4. Nmnat1 is not sufficient to target Wld^S protein to intranuclear foci. C-terminal EGFP fusion constructs transiently transfected into COS cells. (A) Wld^S/EGFP localizes primarily to discrete intranuclear foci (arrowhead), although some remains homogeneously distributed inside the nucleus (arrow). (B) Nmnat1/EGFP is homogeneously distributed, apart from exclusion from nucleoli. N70/EGFP (C) and EGFP (D) alone are homogeneously distributed throughout the cell but EGFP has a preference for the nucleus as previously described (Alonso *et al.*, 2004). Neither is targeted to intranuclear foci. Scale bar, 10 μ m. Figures are representative of three experiments.

nuclear sites, functions that each have potential to influence the strength of the Wld^S phenotype. Thus, Wld^S joins a growing list of chimeric proteins whose biological activity amounts to more than the sum of their parts (Fujimoto *et al.*, 1996; Campbell *et al.*, 1997; Blume-Jensen and Hunter, 2001).

Further studies are needed to test whether VCP binding is required for the neuroprotective Wld^S phenotype, but this possibility was upheld in two important tests. First, Wld^S and VCP show colocalization in at least some DRG neurons known to express the neuroprotective phenotype, as well as in cerebellum where the phenotype *in vivo* remains to be tested. Second, colocalization was conserved across species in DRG of Wld^S rats (Adalbert *et al.*, 2005). The more homogeneous intranuclear distribution of Wld^S in motor neurons *in vivo* makes colocalization in this cell type more difficult to test (Mack *et al.*, 2001; Samsam *et al.*, 2003). Cultured motor neurons electroporated with Wld^S/EGFP show Wld^S puncta without obvious colocalization of VCP but this does not exclude a role for VCP in the neuroprotective phenotype *in vivo* (Supplementary Figure 5).

Colocalization studies cannot ultimately answer the question of whether VCP is required for the Wld^S phenotype. Unfortunately, VCP knockout mice are not available to test the hypothesis and a more complex strategy may be needed. Given the essential role of VCP in endoplasmic reticulum-associated protein degradation (ERAD) and several reports of damaging effects of VCP RNAi, mutation, and deletion in other species or cell lines, it is unlikely that such knockout mice would be viable (Hirabayashi *et al.*, 2001; Kobayashi *et al.*, 2002; Wojcik *et al.*, 2004; Yamanaka *et al.*, 2004). In contrast, Wld^S alters VCP in a way that leaves all cells and organisms healthy, with no overt harmful effect in the orig-

Figure 5. Full-length Wld^S can also partially relocate ubiquitin inside the nucleus. (A) PC12 cells transiently transfected with Wld^S/EGFP fusion construct show a punctate intranuclear distribution (arrowheads), whereas untransfected cells show no signal (arrow). (B) Ubiquitin immunofluorescence shows colocalizing punctate signal in transfected cells (arrowheads), together with a widespread nuclear and cytoplasmic signal. Untransfected cells show only the more homogeneous distribution (arrow). (C) DAPI. (D) Overlay. (E and F) Control experiment in which the first antibody against ubiquitin was omitted. Transfected cells (arrow) show no signal in the red channel. Panel order corresponds to A–D as indicated. Scale bar, 10 μ m. (I–P) A repeat of the experiment in Figure 3 but immunostaining for ubiquitin instead of VCP. Ubiquitin shows the same dependence on N16 for colocalization with Wld^S/DsRed2 in intranuclear spots. (I–L) Transfection with full-length Wld^S/DsRed2 results in partial colocalization, which is retained when the confocal image stack is rotated (arrowheads in L). (M–P) Transfection with N-terminally truncated Wld^S/DsRed2 does not result in colocalization. The small region of overlapping signal (arrow in P) is not retained when the confocal image stack is rotated. (I and M) DAPI staining shows position of nuclei; (J and N) ubiquitin immunostain. (K and O) DsRed2 signal fused, respectively, to full-length Wld^S and Wld^S lacking N16. (L and P) Overlays.



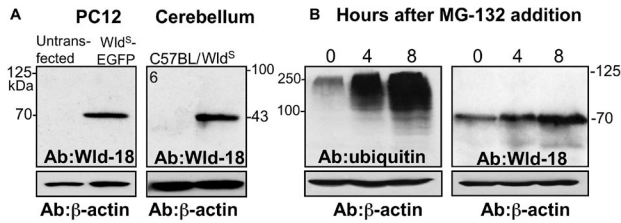


Figure 6. Ubiquitinated Wld^S protein cannot be detected. (A) Western blotting with antibody to Wld^S protein did not detect any ubiquitinated Wld^S/EGFP fusion protein or ubiquitinated Wld^S in transfected PC12 cells (left) or in Wld^S mouse cerebellum (right), respectively. The 70- and 43-kDa bands correspond to the predicted molecular weights of the unmodified proteins. (B) The proteasome inhibitor MG-132 (10 μM for times shown) caused ubiquitination products to build up in PC12 cells (left), but ubiquitinated Wld^S/EGFP (>70 kDa) still could not be detected even on an overexposed ECL (right). Figures are representative two experiments.

inal mutant (Lunn *et al.*, 1989), four lines of transgenic mice (Mack *et al.*, 2001), three of rats (Adalbert *et al.*, 2005) or in double homozygous mice or rats (unpublished observations). This is likely to reflect the confinement of alterations to the nucleus, leaving the essential role of VCP in ERAD unaffected.

Studies in yeast suggest VCP stimulates substrate binding but limits the subsequent growth of a polyubiquitin chain (Richly *et al.*, 2005). However, VCP is dispensable for Ube4b activity when concentrated preparations of protein are used in vitro (Hatakeyama *et al.*, 2001; Mahoney *et al.*, 2002) and in these circumstances removal of the N-terminal 123 amino acids of Ube4b blocks activity for unknown reasons (Mahoney *et al.*, 2002). Our data further highlight the importance of the N-terminus of Ube4b as a regulatory sequence. Many invertebrates lack this sequence but still bind the VCP ortholog Cdc48, so this molecular interaction appears to have changed during evolution.

VCP plays pivotal roles in ERAD, nuclear envelope reconstruction, cell cycle, postmitotic Golgi reassembly, and suppression of apoptosis (Kondo *et al.*, 1997; Dai and Li, 2001; Hetzer *et al.*, 2001; Rabinovich *et al.*, 2002; Wang *et al.*, 2004). Its nuclear functions are equally diverse. First, a nuclear transport role is suggested by its association with adapter proteins Ufd1 and Np14, and by VCP-dependent transport of T-cell-specific adaptor protein into eukaryotic nuclei (Meyer *et al.*, 2000; Marti and King, 2005). Second, VCP controls nucleolar retention of Werner syndrome helicase and its release after DNA damage (Indig *et al.*, 2004). Interestingly, our data fit with the proposal of these authors that other nuclear binding partners regulate VCP distribution and control other pathways. Third, the nucleus has a quality control pathway (Gardner *et al.*, 2005) likely to involve VCP. Interaction and colocalization with expanded polyglutamine and other intranuclear inclusions suggests VCP may be trying to clear misfolded nuclear proteins (Hirabayashi *et al.*, 2001; Doss-Pepe *et al.*, 2003; Mizuno *et al.*, 2003). Finally, VCP regulates the stability of the transcription factor SPT23 (Richly *et al.*, 2005), consistent with the tight regulation of transcription by the UPS (Muratani and Tansey, 2003).

VCP is altered in several neurodegenerative disorders so its interaction with the neuroprotective Wld^S protein is particularly interesting. VCP missense mutations cause inclusion body myopathy with Paget disease of bone and frontotemporal dementia, a disease characterized by ubiquitin-containing nuclear inclusions and white matter pathology (Watts *et al.*, 2004; Schroder *et al.*, 2005). VCP is present in Lewy-like inclusions in amyotrophic lateral sclerosis, in nigral Lewy neurites in Parkinson's disease (Ishigaki *et al.*, 2004), and in ubiquitin-positive intraneuronal inclusions in motor neuron disease with dementia, ballooned neurons in Creutzfeldt-Jakob disease, and dystrophic neurites of senile plaque in Alzheimer's disease (Mizuno *et al.*, 2003). In polyglutamine disorders such as Huntington's disease and Machado-Joseph disease, specific binding to expanded polyglutamine targets VCP to intranuclear inclusions (Hiraba-

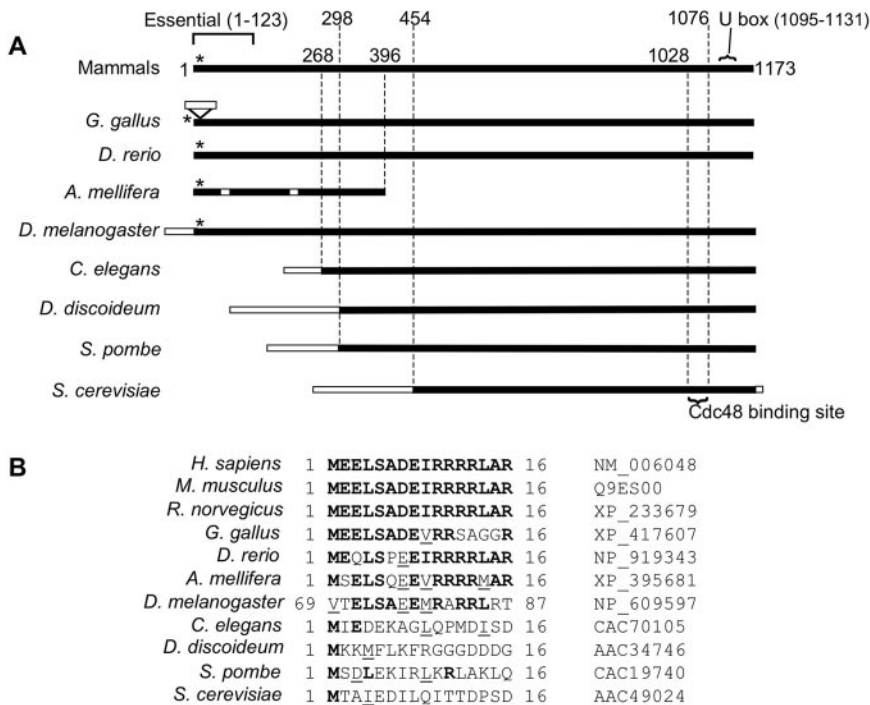


Figure 7. VCP binding to N16 is an evolutionary "recent" event. (A) Full-length alignment of Ube4b and Ufd2 sequences. (B) Amino acid alignment of N16-like or other N-terminal sequences in the same proteins. The database accession numbers are also shown. Mammals, birds, fish, and insects have sequence showing significant homology to the VCP binding site in N16 at positions denoted by the asterisk (*). Nematodes, slime molds, and yeasts lack the entire N-terminal extension containing this sequence. The Cdc48 binding site of *S. cerevisiae* Ufd2p (Richly *et al.*, 2005), the U box (Hatakeyama *et al.*, 2001), and the sequence essential for in vitro ubiquitination activity (Mahoney *et al.*, 2002) are also marked. Black boxes, regions of significant homology to human Ube4b; open boxes, regions not homologous to human Ube4b; bold, amino acids identical to human Ube4b; underlined, conservative substitutions.

yashi *et al.*, 2001). This interaction appears to influence disease severity, as loss-of-function mutations in the *Drosophila* VCP ortholog, *ter4*, dominantly suppress neurodegeneration caused by expanded polyglutamine (Higashiyama *et al.*, 2002).

It is now important to determine whether Wld^S protein, or N70 can interfere with the effect of VCP in any of these neurodegenerative disorders. Ectopic expression in *Drosophila* of mammalian Ube4b suppresses polyglutamine disease, and loss of function mutations in VCP have a similar effect (Higashiyama *et al.*, 2002; Matsumoto *et al.*, 2004). It is also now clear that Wld^S and expanded polyglutamine both bind VCP directly and partially relocalize it to intranuclear foci (Hirabayashi *et al.*, 2001). Taken together, these observations raise the intriguing possibility that N70 and VCP antagonize each other in some circumstances as a result of the binding interaction we describe.

In summary, we report direct interaction between VCP and the N-terminal 16 amino acids of both Wld^S and Ube4b proteins. This interaction drives focal intranuclear clustering of VCP in Wld^S neurons, probably together with associated multiubiquitinated proteins, and helps understand the function of an important, evolutionarily recent regulatory sequence in the Ube4b protein. It is now important to determine whether the redistribution of covalently attached Nmnat1 or of bound VCP influences the strength of the Wld^S phenotype in vivo and to understand how the N-terminal binding of VCP to Ube4b influences this ubiquitin ligase.

ACKNOWLEDGMENTS

We thank Prof. Akira Kakizuka (Kyoto University) for the "TV" PC12 cell line stably transfected with VCP/EGFP fusion construct; Dr. Sarah Spinette, Professor James Mahoney, and Professor Antony Rosen (Johns Hopkins) for purified VCP and human Ube4b cDNA; and Rita Lange for mouse fibroblast cDNA library. We thank Dr. Thorsten Hoppe (University of Hamburg) for helpful discussion and Dr. Jonathan Gilley (Babraham Institute) for practical assistance. This work was funded primarily by Deutsche Forschungsgemeinschaft Grant CO 276/1-1 and by the Biotechnology and Biological Sciences Research Council. Additional funding came from the Federal Ministry of Education and Research (FKZ; Grant 01 KS 9502) and Center for Molecular Medicine, University of Cologne (CMMC), the Wellcome Trust, the Medical Research Council, the Amyotrophic Lateral Sclerosis Association and Koeln Fortune.

REFERENCES

Adalbert, R. *et al.* (2005). A rat model of slow Wallerian degeneration (Wld^S) with improved preservation of neuromuscular synapses. *Eur. J. Neurosci.* *21*, 271–277.

Alonso, M. B. *et al.* (2004). Identification and characterization of ZFP-57, a novel zinc finger transcription factor in the mammalian peripheral nervous system. *J. Biol. Chem.* *279*, 25653–25664.

Anderson, R. M., Bitterman, K. J., Wood, J. G., Medvedik, O., Cohen, H., Lin, S. S., Manchester, J. K., Gordon, J. I., and Sinclair, D. A. (2002). Manipulation of a nuclear NAD⁺ salvage pathway delays aging without altering steady-state NAD⁺ levels. *J. Biol. Chem.* *277*, 18881–18890.

Araki, T., Sasaki, Y., and Milbrandt, J. (2004). Increased nuclear NAD biosynthesis and SIRT1 activation prevent axonal degeneration. *Science* *305*, 1010–1013.

Blume-Jensen, P., and Hunter, T. (2001). Oncogenic kinase signalling. *Nature* *411*, 355–365.

Campbell, R. K., Bergert, E. R., Wang, Y., Morris, J. C., and Moyle, W. R. (1997). Chimeric proteins can exceed the sum of their parts: implications for evolution and protein design. *Nat. Biotechnol.* *15*, 439–443.

Coleman, M. P. (2005). Axon degeneration mechanisms: commonality amid diversity. *Nat. Rev. Neurosci.* *6*, 889–898.

Coleman, M. P., and Perry, V. H. (2002). Axon pathology in neurological disease: a neglected therapeutic target. *Trends Neurosci.* *25*, 532–537.

Coleman, M. P., and Ribchester, R. R. (2004). Programmed axon death, synaptic dysfunction and the ubiquitin proteasome system. *Curr. Drug Targets CNS Neurol. Disord.* *3*, 227–238.

Conforti, L., Tarlton, A., Mack, T. G., Mi, W., Buckmaster, E. A., Wagner, D., Perry, V. H., and Coleman, M. P. (2000). A Ufd2/D4Cole1e chimeric protein and overexpression of *rbp7* in the slow wallerian degeneration (Wld^S) mouse. *Proc. Natl. Acad. Sci. USA* *97*, 11377–11382.

Crawford, T. O., Hsieh, S. T., Schryer, B. L., and Glass, J. D. (1995). Prolonged axonal survival in transected nerves of C57BL/Ola mice is independent of age. *J. Neurocytol.* *24*, 333–340.

Dai, R. M., Chen, E., Longo, D. L., Gorbea, C. M., and Li, C. C. (1998). Involvement of valosin-containing protein, an ATPase Co-purified with IkappaBalpha and 26 S proteasome, in ubiquitin-proteasome-mediated degradation of IkappaBalpha. *J. Biol. Chem.* *273*, 3562–3573.

Dai, R. M., and Li, C. C. (2001). Valosin-containing protein is a multi-ubiquitin chain-targeting factor required in ubiquitin-proteasome degradation. *Nat. Cell Biol.* *3*, 740–744.

Doss-Pepe, E. W., Stenroos, E. S., Johnson, W. G., and Madura, K. (2003). Ataxin-3 interactions with rad23 and valosin-containing protein and its associations with ubiquitin chains and the proteasome are consistent with a role in ubiquitin-mediated proteolysis. *Mol. Cell Biol.* *23*, 6469–6483.

Emanuelli, M., Carnevali, F., Saccucci, F., Pierella, F., Amici, A., Raffaelli, N., and Magni, G. (2001). Human NMN adenylyltransferase: molecular cloning, chromosomal localization, tissue mRNA levels, bacterial expression, and enzymatic properties. *J. Biol. Chem.* *276*, 406–412.

Ferri, A., Sanes, J. R., Coleman, M. P., Cunningham, J. M., and Kato, A. C. (2003). Inhibiting axon degeneration and synapse loss attenuates apoptosis and disease progression in a mouse model of motoneuron disease. *Curr. Biol.* *13*, 669–673.

Fujimoto, J., Shiota, M., Iwahara, T., Seki, N., Satoh, H., Mori, S., and Yamamoto, T. (1996). Characterization of the transforming activity of p80, a hyperphosphorylated protein in a Ki-1 lymphoma cell line with chromosomal translocation t(2;5). *Proc. Natl. Acad. Sci. USA* *93*, 4181–4186.

Gardner, R. G., Nelson, Z. W., and Gottschling, D. E. (2005). Degradation-mediated protein quality control in the nucleus. *Cell* *120*, 803–815.

Hatakeyama, S., Yada, M., Matsumoto, M., Ishida, N., and Nakayama, K. I. (2001). U-Box proteins as a new family of ubiquitin-protein ligases. *J. Biol. Chem.* *276*, 32111–32120.

Henderson, C. E., Bloch-Gallego, E., and Camu, W. (1995). Purified embryonic motoneurons. In: *Nerve Cell Culture: A Practical Approach*, ed. J. Cohen and G. Wilkin, London: Oxford University Press, 69–81.

Hetzer, M., Meyer, H. H., Walther, T. C., Bilbao-Cortes, D., Warren, G., and Mattaj, I. W. (2001). Distinct AAA-ATPase p97 complexes function in discrete steps of nuclear assembly. *Nat. Cell Biol.* *3*, 1086–1091.

Higashiyama, H., Hirose, F., Yamaguchi, M., Inoue, Y. H., Fujikake, N., Matsukage, A., and Kakizuka, A. (2002). Identification of *ter94*, *Drosophila* VCP, as a modulator of polyglutamine-induced neurodegeneration. *Cell Death Differ.* *9*, 264–273.

Hirabayashi, M. *et al.* (2001). VCP/p97 in abnormal protein aggregates, cytoplasmic vacuoles, and cell death, phenotypes relevant to neurodegeneration. *Cell Death Differ.* *8*, 977–984.

Hoppe, T. (2005). Multiubiquitylation by E4 enzymes: 'one size' doesn't fit all. *Trends Biochem. Sci.* *30*, 183–187.

Hoppe, T., Cassata, G., Barral, J. M., Springer, W., Hutagalung, A. H., Epstein, H. F., and Baumeister, R. (2004). Regulation of the myosin-directed chaperone UNC-45 by a novel E3/E4-multiubiquitylation complex in *C. elegans*. *Cell* *118*, 337–349.

Indig, F. E., Partridge, J. J., Kobbe Cv, C., Aladjem, M. I., Latterich, M., and Bohr, V. A. (2004). Werner syndrome protein directly binds to the AAA ATPase p97/VCP in an ATP-dependent fashion. *J. Struct. Biol.* *146*, 251–259.

Ishigaki, S., Hishikawa, N., Niwa, J., Iemura, S., Natsume, T., Hori, S., Kakizuka, A., Tanaka, K., and Sobue, G. (2004). Physical and functional interaction between Dofrin and Valosin-containing protein that are colocalized in ubiquitylated inclusions in neurodegenerative disorders. *J. Biol. Chem.* *279*, 51376–51385.

Jarosch, E., Taxis, C., Volkwein, C., Bordallo, J., Finley, D., Wolf, D. H., and Sommer, T. (2002). Protein dislocation from the ER requires polyubiquitination and the AAA-ATPase Cdc48. *Nat. Cell Biol.* *4*, 134–139.

Kaneko, C., Hatakeyama, S., Matsumoto, M., Yada, M., Nakayama, K., and Nakayama, K. I. (2003). Characterization of the mouse gene for the U-box-type ubiquitin ligase UFD2a. *Biochem. Biophys. Res. Commun.* *300*, 297–304.

- Kerschensteiner, M., Schwab, M. E., Lichtman, J. W., and Misgeld, T. (2005). In vivo imaging of axonal degeneration and regeneration in the injured spinal cord. *Nat. Med.* *11*, 572–577.
- Kobayashi, T., Tanaka, K., Inoue, K., and Kakizuka, A. (2002). Functional ATPase activity of p97/valosin-containing protein (VCP) is required for the quality control of endoplasmic reticulum in neuronally differentiated mammalian PC12 cells. *J. Biol. Chem.* *277*, 47358–47365.
- Koegl, M., Hoppe, T., Schlenker, S., Ulrich, H. D., Mayer, T. U., and Jentsch, S. (1999). A novel ubiquitination factor, E4, is involved in multiubiquitin chain assembly. *Cell* *96*, 635–644.
- Kondo, H., Rabouille, C., Newman, R., Levine, T. P., Pappin, D., Freemont, P., and Warren, G. (1997). p47 is a cofactor for p97-mediated membrane fusion. *Nature* *388*, 75–78.
- Krona, C., Ejeskar, K., Abel, F., Kogner, P., Bjelke, J., Bjork, E., Sjoberg, R. M., and Martinsson, T. (2003). Screening for gene mutations in a 500 kb neuroblastoma tumor suppressor candidate region in chromosome 1p; mutation and stage-specific expression in UBE4B/UFD2. *Oncogene* *22*, 2343–2351.
- Lunn, E. R., Perry, V. H., Brown, M. C., Rosen, H., and Gordon, S. (1989). Absence of Wallerian degeneration does not hinder regeneration in peripheral nerve. *Eur. J. Neurosci.* *1*, 27–33.
- Macinnis, B. L., and Campenot, R. B. (2005). Regulation of Wallerian degeneration and nerve growth factor withdrawal-induced pruning of axons of sympathetic neurons by the proteasome and the MEK/Erk pathway. *Mol. Cell Neurosci.* *28*, 430–439.
- Mack, T. G. *et al.* (2001). Wallerian degeneration of injured axons and synapses is delayed by a Ube4b/Nmnat chimeric gene. *Nat. Neurosci.* *4*, 1199–1206.
- Magni, G., Amici, A., Emanuelli, M., Orsomando, G., Raffaelli, N., and Ruggieri, S. (2004). Structure and function of nicotinamide mononucleotide adenylyltransferase. *Curr. Med. Chem.* *11*, 873–885.
- Mahoney, J. A., Odin, J. A., White, S. M., Shaffer, D., Koff, A., Casciola-Rosen, L., and Rosen, A. (2002). The human homologue of the yeast polyubiquitination factor Ufd2p is cleaved by caspase 6 and granzyme B during apoptosis. *Biochem. J.* *361*, 587–595.
- Marti, F., and King, P. D. (2005). The p95–100 kDa ligand of the T cell-specific adaptor (TSAd) protein Src-homology-2 (SH2) domain implicated in TSAd nuclear import is p97 Valosin-containing protein (VCP). *Immunol. Lett.* *97*, 235–243.
- Matsumoto, M., Yada, M., Hatakeyama, S., Ishimoto, H., Tanimura, T., Tsuji, S., Kakizuka, A., Kitagawa, M., and Nakayama, K. I. (2004). Molecular clearance of ataxin-3 is regulated by a mammalian E4. *EMBO J.* *23*, 659–669.
- Meyer, H. H., Shorter, J. G., Seemann, J., Pappin, D., and Warren, G. (2000). A complex of mammalian ufd1 and npl4 links the AAA-ATPase, p97, to ubiquitin and nuclear transport pathways. *EMBO J.* *19*, 2181–2192.
- Mi, W., Beirowski, B., Gillingwater, T. H., Adalbert, R., Wagner, D., Grumme, D., Osaka, H., Conforti, L., Arnhold, S., Addicks, K., Wada, K., Ribchester, R. R., and Coleman, M. P. (2005). The slow Wallerian degeneration gene, WldS, inhibits axonal spheroid pathology in gracile axonal dystrophy mice. *Brain* *128*, 405–416.
- Mizuno, Y., Hori, S., Kakizuka, A., and Okamoto, K. (2003). Vacuole-creating protein in neurodegenerative diseases in humans. *Neurosci. Lett.* *343*, 77–80.
- Mogk, A., Dougan, D., Weibezahn, J., Schlieker, C., Turgay, K., and Bukau, B. (2004). Broad yet high substrate specificity: the challenge of AAA+ proteins. *J. Struct. Biol.* *146*, 90–98.
- Muratani, M., and Tansey, W. P. (2003). How the ubiquitin-proteasome system controls transcription. *Nat. Rev. Mol. Cell Biol.* *4*, 192–201.
- Okumura, F., Hatakeyama, S., Matsumoto, M., Kamura, T., and Nakayama, K. I. (2004). Functional regulation of FEZ1 by the U-box-type ubiquitin ligase E4B contributes to neurogenesis. *J. Biol. Chem.* *279*, 53533–53543.
- Rabinovich, E., Kerem, A., Frohlich, K. U., Diamant, N., and Bar-Nun, S. (2002). AAA-ATPase p97/Cdc48p, a cytosolic chaperone required for endoplasmic reticulum-associated protein degradation. *Mol. Cell Biol.* *22*, 626–634.
- Raffaelli, N., Sorci, L., Amici, A., Emanuelli, M., Mazzola, F., and Magni, G. (2002). Identification of a novel human nicotinamide mononucleotide adenylyltransferase. *Biochem. Biophys. Res. Commun.* *297*, 835–840.
- Raoul, C., Estevez, A. G., Nishimune, H., Cleveland, D. W., deLapeyriere, O., Henderson, C. E., Haase, G., and Pettmann, B. (2002). Motoneuron death triggered by a specific pathway downstream of Fas potentiation by ALS-linked SOD1 mutations. *Neuron* *35*, 1067–1083.
- Richly, H., Rape, M., Braun, S., Rumpf, S., Hoegge, C., and Jentsch, S. (2005). A series of ubiquitin binding factors connects CDC48/p97 to substrate multiubiquitylation and proteasomal targeting. *Cell* *120*, 73–84.
- Sajadi, A., Schneider, B. L., and Aebischer, P. (2004). Wld(s)-mediated protection of dopaminergic fibers in an animal model of Parkinson disease. *Curr. Biol.* *14*, 326–330.
- Samsam, M., Mi, W., Wessig, C., Zielasek, J., Toyka, K. V., Coleman, M. P., and Martini, R. (2003). The Wlds mutation delays robust loss of motor and sensory axons in a genetic model for myelin-related axonopathy. *J. Neurosci.* *23*, 2833–2839.
- Schroder, R., Watts, G. D., Mehta, S. G., Evert, B. O., Broich, P., Fliessbach, K., Pauls, K., Hans, V. H., Kimonis, V., and Thal, D. R. (2005). Mutant valosin-containing protein causes a novel type of frontotemporal dementia. *Ann. Neurol.* *57*, 457–461.
- Spinette, S., Lengauer, C., Mahoney, J. A., Jallepalli, P. V., Wang, Z., Casciola-Rosen, L., and Rosen, A. (2004). Ufd2, a novel autoantigen in scleroderma, regulates sister chromatid separation. *Cell Cycle* *3*, 1638–1644.
- Wang, J., Zhai, Q., Chen, Y., Lin, E., Gu, W., McBurney, M. W., and He, Z. (2005). A local mechanism mediates NAD-dependent protection of axon degeneration. *J. Cell Biol.* *170*, 349–355.
- Wang, M. S., Davis, A. A., Culver, D. G., and Glass, J. D. (2002). WldS mice are resistant to paclitaxel (taxol) neuropathy. *Ann. Neurol.* *52*, 442–447.
- Wang, Q., Song, C., and Li, C. C. (2004). Molecular perspectives on p97-VCP: progress in understanding its structure and diverse biological functions. *J. Struct. Biol.* *146*, 44–57.
- Watts, G. D., Wymer, J., Kovach, M. J., Mehta, S. G., Mumm, S., Darvish, D., Pestronk, A., Whyte, M. P., and Kimonis, V. E. (2004). Inclusion body myopathy associated with Paget disease of bone and frontotemporal dementia is caused by mutant valosin-containing protein. *Nat. Genet.* *36*, 377–381.
- Wojcik, C., Yano, M., and DeMartino, G. N. (2004). RNA interference of valosin-containing protein (VCP/p97) reveals multiple cellular roles linked to ubiquitin/proteasome-dependent proteolysis. *J. Cell Sci.* *117*, 281–292.
- Wu, R., Terry, A. V., Singh, P. B., and Gilbert, D. M. (2005). Differential subnuclear localization and replication timing of histone H3 lysine 9 methylation states. *Mol. Biol. Cell* *16*, 2872–2881.
- Yamanaka, K., Okubo, Y., Suzaki, T., and Ogura, T. (2004). Analysis of the two p97/VCP/Cdc48p proteins of *Caenorhabditis elegans* and their suppression of polyglutamine-induced protein aggregation. *J. Struct. Biol.* *146*, 242–250.
- Zhai, Q., Wang, J., Kim, A., Liu, Q., Watts, R., Hoopfer, E., Mitchison, T., Luo, L., and He, Z. (2003). Involvement of the ubiquitin-proteasome system in the early stages of wallerian degeneration. *Neuron* *39*, 217–225.